

On the discrepancies in the low energy neutron-deuteron breakup

H. Witała

*M. Smoluchowski Institute of Physics,
Jagiellonian University, PL-30059 Kraków, Poland*

W. Glöckle

Institut für theoretische Physik II, Ruhr-Universität Bochum, D-44780 Bochum, Germany

(Dated: September 14, 2021)

Abstract

In view of recent neutron-deuteron (nd) breakup data for neutron-neutron (nn) and neutron-proton (np) quasi-free-scattering (QFS) arrangements and the large discrepancy found between theoretical predictions and measured nn QFS cross sections, we analyze the sensitivity of the QFS cross sections to different partial wave components of the nucleon-nucleon (NN) interaction. We found that the QFS cross section is strongly dominated by the 1S_0 and $^3S_1 - ^3D_1$ contributions. Because the standard three-nucleon force (3NF) only weakly influence the QFS region, we conjecture, that it must be the nn 1S_0 force component which is responsible for the discrepancy in the nn QFS peak. A stronger 1S_0 nn force is required to bring theory and data into agreement. Such an increased strength of the nn interaction will, however, not help to explain the nd breakup symmetric-space-star (SST) discrepancy. Further experimental cross-checkings are required.

PACS numbers: 21.45.-v, 21.45.Bc, 25.10.+s, 25.40.Cm

I. INTRODUCTION

The study of the nucleon induced deuteron breakup is a powerful tool to test the nuclear Hamiltonian [1]. By comparing theoretical predictions to breakup data in different configurations of the outgoing nucleons not only the present day models of two-nucleon (2N) interactions can be tested but also effects of three-nucleon forces (3NF) can be studied [2, 3].

Despite spectacular successes in interpreting some breakup data based on a 3N Hamiltonian with free NN interactions supplemented by genuine 3NF's [1, 2, 3], some clear cut discrepancies between theory and data exist and require further theoretical and experimental studies. Those discrepancies can be divided into ones occurring at low and at higher energies. The last ones occur at energies of the incoming nucleon above $E_N^{lab} \approx 100$ MeV and since the 3NF effects in the 3N continuum increase with energy [2, 3] they can be probably traced back to neglected short-range terms of the 3NF. Also in some specific phase-space regions of the Nd breakup effects of relativity can play a role [4, 5, 6]

Low energy discrepancies were found in proton-deuteron (pd) and neutron-deuteron (nd) breakup in some particular kinematical arrangements of the outgoing three nucleons [1, 7, 8, 9, 10, 11, 12, 13, 14, 15, 16, 17, 18, 19]. The strongest discrepancies between theoretical cross sections and data occur in the nn QFS [10, 11, 16] and in the symmetrical nd space star (SST) [7, 8, 9, 12, 13, 14, 15] geometries.

In the SST configuration three nucleons are flying away in the plane perpendicular to the incoming beam in the c.m. system with momenta of equal magnitude and a pairwise angular separation of 120 degrees. The low energy pd SST cross sections [17, 18, 19, 20] are slightly overestimated and the nd SST cross sections [7, 8, 9, 12, 13, 14, 15] are clearly underestimated by pure nd (the pp Coulomb force neglected) theoretical predictions. The theoretical cross sections practically do not depend on the NN potential used in the calculations [1, 3]. They also do not change significantly if any of the present day 3NF models is included [1, 3]. The observed diminishing of the disagreement between nd theory and pd SST data with increasing proton energy: [18] ($E_p^{lab} = 13$ MeV), [19] ($E_p^{lab} = 19$ MeV), and [20] ($E_p^{lab} = 65$ MeV), leading to a quite good description of the 65 MeV pd data [20], led to the conclusion, that probably the neglected pp Coulomb force is responsible for the low energy pd SST cross section discrepancies. However, recent breakup calculations with the long-range Coulomb force included revealed only a small lowering of the SST cross section by the pp Coulomb force [21]. Much larger discrepancies up to $\approx 30\%$ have been found for the nd SST. The data come from independent measurements, performed

at the same energy and with different experimental arrangements: $E_n^{lab} = 10.3$ MeV [12, 13, 14], $E_n^{lab} = 13$ MeV [7, 8, 9], $E_n^{lab} = 16$ MeV [15].

The QFS refers to a situation where one of the nucleons is at rest in the laboratory system. In the pd breakup the np or pp QFS configurations are possible, while for the nd breakup np or nn can form a quasi-freely scattered pair. The cross sections for pp QFS in pd breakup: [18] ($E_p^{lab} = 13$ MeV), [19] ($E_p^{lab} = 19$ MeV), and [22] ($E_p^{lab} = 65$ MeV), and for nn QFS: [10] ($E_n^{lab} = 26$ MeV), [11] ($E_n^{lab} = 25$ MeV), and [16] ($E_n^{lab} = 10.31$ MeV), and np QFS [10] in nd breakup have been measured and the picture resembles that for SST: also here the pp QFS cross sections are overestimated by the nd theory while the nn QFS cross sections are clearly underestimated by $\approx 20\%$. Suprisingly, when instead of the nn pair the np pair is quasi-freely scattered, the theory follows nicely the np QFS cross section data taken in the nd breakup measurement [10]. Also the nd theory provides QFS cross sections which are highly independent from the realistic NN potential used in the calculations and they practically do not change when any of the present day 3NF's is included [1, 3]. Again, the discrepancies between nd theory and pp QFS cross sections diminish with increasing energy [18, 19, 22], indicating that the neglected pp Coulomb force is probably responsible for them. Also here the pd breakup calculations show that the pp Coulomb force only slightly lowers the nd theory in the pp QFS region [21].

The good description of the np QFS cross section data from the $E_n^{lab} = 26$ MeV nd breakup measurement [10] contrasts with the drastic discrepancy to the nn QFS cross section data taken in the same experiment [10]. This prompted us to look closely how different NN force components contribute to QFS cross sections. This is outlined in section II, while section III deals with the SST cross sections. We summarize in section IV.

II. SENSITIVITY TEST FOR QFS CROSS SECTIONS

The tests are performed using the (semi)phenomenological NN potentials alone (AV18 [23], CD Bonn [24], Nijm1 and Nijm2 [25]) or combining them with the 2π -exchange TM99 3NF [26, 27]. For details of our approach to solve the 3N Faddeev equation, which is based on momentum space partial wave decomposition, we refer to [1, 28]. As an example we checked that at the energy $E_n^{lab} = 26$ MeV the np and nn QFS cross section are practically insensitive to the exchange between different realistic NN potentials and that the effects of 3NF's are negligible (see Fig. 1 and 2).

In Fig. 1 we show the cross section $d^5\sigma/d\Omega_1 d\Omega_2 dS$ for the nd breakup reaction $d(n, N_1 N_2) N_3$

under exact QFS condition ($\vec{p}_3^{lab} = 0$) as a function of the laboratory angle θ_1 of the outgoing nucleon N_1 . In Fig. 2 we show nn and np QFS cross sections for configurations measured in Ref. [10]. Since the QFS cross section is practically insensitive to the action of a 3NF the reason for the nearly 20% underestimation of the nn QFS cross section data found in [10] must be traced to the underlying NN force. At low energy the largest contribution should be provided by the S-wave components of the NN potential. In case of free np and nn scattering these are the $^1S_0(\text{np}) + ^3S_1 - ^3D_1$ and $^1S_0(\text{nn})$ contributions, respectively. For the nd breakup and np or nn QFS configurations that dominance can also be expected. However, due to the presence of an additional nucleon in the incoming deuteron, for nn QFS also a smaller contribution from the $^3S_1 - ^3D_1$ np interaction is possible. In Figs. 3 and 4 we show contributions to the np and nn QFS cross sections from 1S_0 , $^3S_1 - ^3D_1$, and from all other components of the NN interaction up to a two-body total angular momentum $j = 5$. It is clearly seen, that at low energies the QFS peak is build predominantly from 1S_0 and 3S_1 components, with practically negligible contributions from higher angular momentum states. It is also seen that quite different pictures arise for np and nn QFS. While for np QFS $^3S_1 - ^3D_1$ is the most dominant contribution, for nn QFS it is the 1S_0 force which contributes decisively. If the disagreement between data and theory in the nn QFS peak has its source in one or both of these two force components it must be the 1S_0 nn force. The 1S_0 nn force is determined up to now only indirectly due to lack of free nn data. Both 1S_0 and $^3S_1 - ^3D_1$ np forces are well determined by np scattering data and by the deuteron properties. Also the agreement for np QFS found in [10] further supports the possibility of a wrong nn 1S_0 interaction. Namely if QFS resembles free nucleon-nucleon scattering then the 1S_0 contribution to the nn QFS should be mostly of the 1S_0 nn type whereas the 1S_0 contribution to the np QFS is mostly given by the 1S_0 np force component. That would imply that the nn QFS is a powerfull tool to study 1S_0 nn force component. Our numerical studies revealed, that at low energies higher order rescatterings are important. As a result quasi-free-scattering does not resemble exactly free scattering and in the nn QFS peak also contributions from $^3S_1 - ^3D_1$ and 1S_0 np are present as well as in the np QFS peak there is also a small admixture from 1S_0 nn together with admixture in both, nn and np QFS's, from higher partial wave components. Nevertheless the low energy dominance of the 1S_0 nn contribution in the nn QFS peak and the dominance of the 1S_0 and $^3S_1 - ^3D_1$ np forces in the np QFS peak remains true also in the presence of rescatterings.

That indeed the nn QFS is extremely sensitive to the 1S_0 nn force component we demonstrate in Figs. 5 and 6 by showing the changes of the QFS cross section induced by changes of the nn 1S_0 interaction. In this study we chose a very simple device for that change, namely multiplying the

1S_0 nn matrix element of the CD Bonn potential by a factor λ . The result is, that the nn QFS undergoes significant variations while the np QFS cross sections are practically unchanged.

Going to higher energies the QFS cross sections become sensitive also to higher angular momentum components of the NN interaction and the dominance of S-waves is lost. Also the sensitivity of the nn QFS peak to changes of the 1S_0 nn interaction is significantly reduced. This is demonstrated in Figs. 7 and 8 at $E_n^{lab} = 65$ MeV.

One can ask which change of the 1S_0 nn force is required to bring the nn QFS theoretical cross sections into agreement with the data. To remove the 18% discrepancy found in [10] for nn QFS would require a value of $\lambda \approx 1.08$. Such an increased strength of the 1S_0 nn interaction would drastically decrease 1S_0 nn scattering length a_{nn} to $a_{nn}^{^1S_0}(\lambda = 1.08) = -135$ fm and would lead to a nearly bound state of two neutrons.

III. SENSITIVITY TEST FOR SST CROSS SECTIONS

Here we perform corresponding studies for the nd SST break up configuration. Even such a drastic increase of the nn 1S_0 force strength by a factor $\lambda \approx 1.08$ would not remove the discrepancy for the nd SST configuration. Also here the main contributions to the cross section come from the 1S_0 and $^3S_1 - ^3D_1$ components. Contrary to nn QFS here the $^3S_1 - ^3D_1$ is the dominant component. The building up of the SST cross sections in $E_n^{lab} = 26$ MeV and $E_n^{lab} = 13$ MeV nd breakup by components of the NN force is shown in the upper panels of Figs. 9 and 10, respectively, and the sensitivity to the nn 1S_0 force in the lower panels of Figs. 9 and 10. It is seen that changes which would provide an explanation for the nn QFS have practically no effect on the SST discrepancy.

IV. SUMMARY

Summarizing, the QFS Nd breakup cross sections are influenced only slightly by present day 3NF's. Thus they are not responsible for the large differences between theoretical predictions and data found for the nd breakup nn QFS cross sections. The study of the sensitivity of these cross sections to different NN force components has shown, that in order to explain these discrepancies a stronger nn 1S_0 force is required, leading however in our simplistic modification to an unrealistic nn scattering length. The SST discrepancy is even more serious. Further measurements are required to solidify the experimental situation.

Acknowledgments

This work was supported by the Polish 2008-2011 science funds as the research project No. N N202 077435. It was also partially supported by the Helmholtz Association through funds provided to the virtual institute “Spin and strong QCD”(VH-VI-231) and by the European Community-Research Infrastructure Integrating Activity “Study of Strongly Interacting Matter” (acronym HadronPhysics2, Grant Agreement n. 227431) under the Seventh Framework Programme of EU. The numerical calculations have been performed on the supercomputer cluster of the JSC, Jülich, Germany.

-
- [1] W. Glöckle, H. Witała, D. Hüber, H. Kamada, J. Golak, Phys. Rep. **274**, 107 (1996).
 - [2] H. Witała, W. Glöckle, J. Golak, A. Nogga, H.Kamada, R. Skibiński, J. Kuroś-Żołnierczuk, Phys. Rev. **C63**, 024007 (2001).
 - [3] J. Kuroś-Żołnierczuk, H. Witała, J. Golak, H.Kamada, A. Nogga, R. Skibiński, W. Glöckle, Phys. Rev. **C66**, 024004 (2002).
 - [4] H. Witała, J. Golak, W. Glöckle, H. Kamada, Phys. Rev. **C71**, 054001 (2005).
 - [5] H.Witała, J. Golak, and R. Skibiński, Phys. Lett. **B 634**, 374 (2006).
 - [6] R. Skibiński, H. Witała, J. Golak, Eur. Phys. J. **A 30**, 369 (2006).
 - [7] H. R. Setze et al., Phys. Lett. **B388**, 229 (1996).
 - [8] H. R. Setze et al., Phys. Rev. **C71**, 034006 (2005).
 - [9] J. Strate et al., Nucl. Phys. **A501**, 51 (1989).
 - [10] A. Siepe et al., Phys. Rev. **C65**, 034010 (2002).
 - [11] X.C. Ruan et al., Phys. Rev. **C75**, 057001 (2002).
 - [12] M. Stephan et al., Phys. Rev. **C39**, 2133 (1989).
 - [13] K. Gerbhard et al., Nucl. Phys. **A561**, 232 (1993).
 - [14] S. Chuchwell et al., TUNL Progress Report **XL**, 26 (2001).
 - [15] S. Chuchwell et al., TUNL Progress Report **XL**, 30 (2001).
 - [16] W. Lübbcke, Ph.D. thesis, University Bochum, 1992.
 - [17] Y. Tachikawa et al., Nucl. Phys. **A684**, 583c (2001).
 - [18] G. Rauprich et al., Nucl. Phys. **A535**, 313 (1991).
 - [19] H. Patberg et al., Phys. Rev. **C53**, 1497 (1996).
 - [20] J. Zejma et al., Phys. Rev. **C55**, 42 (1997).
 - [21] A. Deltuva, A. C. Fonseca, and P. U. Sauer, Phys. Rev. **C72**, 054004 (2005).
 - [22] M. Allet et al., Few-Body Systems **20**, 27 (1996).
 - [23] R. B. Wiringa, V. G. J. Stoks, R. Schiavilla, Phys. Rev. **C51**, 38 (1995).

- [24] R. Machleidt, F. Sammarruca, and Y. Song, Phys. Rev. C **53**, R1483 (1996).
- [25] V. G. J. Stoks *et al.*, Phys. Rev. C **49**, 2950 (1994).
- [26] S.A. Coon *et al.*, Nucl. Phys. **A317**, 242 (1979); S. A. Coon, W. Glöckle, Phys. Rev. C **23**, 1970 (1981).
- [27] S. A. Coon and H. K. Han, Few Body Syst., **30**, 131 (2001).
- [28] W. Glöckle, The Quantum Mechanical Few-Body Problem, Springer Verlag 1983.

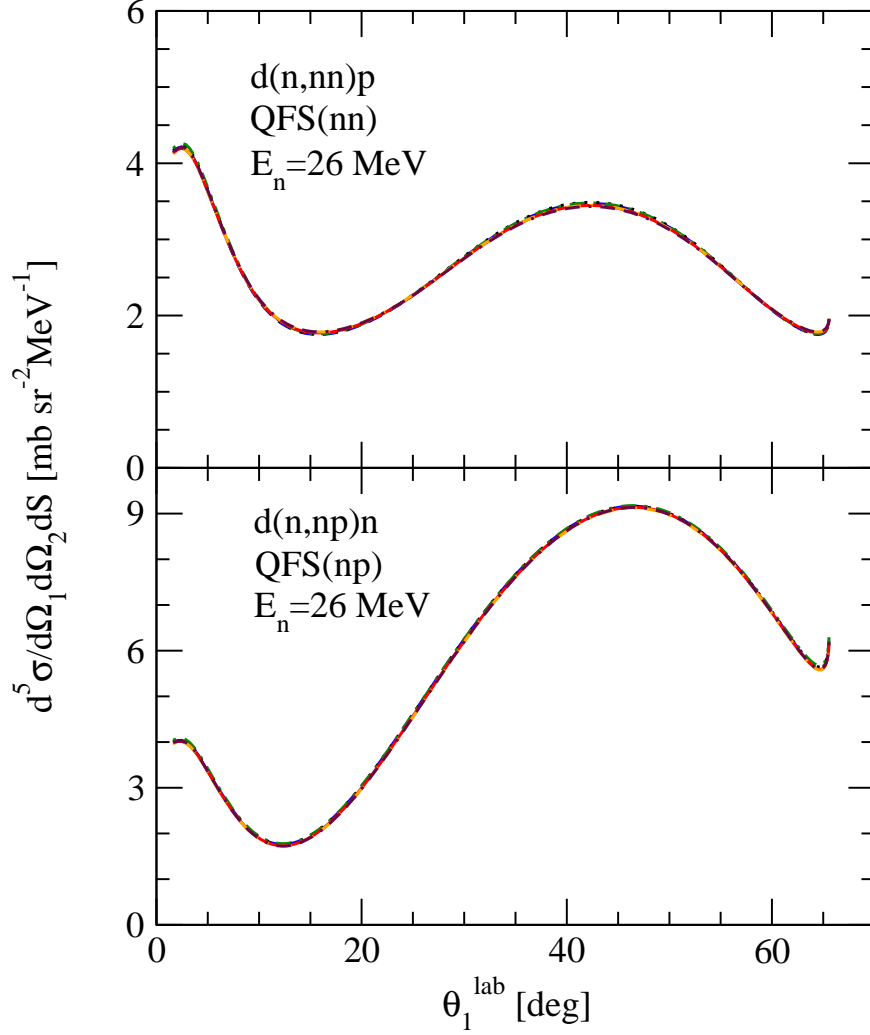


FIG. 1: (color online) The cross section $d^5\sigma/d\Omega_1 d\Omega_2 dS$ for the $E_n^{\text{lab}} = 26 \text{ MeV}$ nd breakup reaction $d(n,nn)p$ (upper panel) and $d(n,np)n$ (lower panel) under exact QFS condition (the momentum of the undetected third nucleon $\vec{p}_3^{\text{lab}} = 0$: nn QFS for the upper and np QFS for the lower panel) as a function of the laboratory angle of the detected neutron. The (overlapping) lines correspond to different underlying dynamics: CD Bonn - dashed (blue), Nijm I - dotted (black), Nijm II - dashed-dotted (green), CD Bonn+TM99 - solid (red), Nijm I + TM99 - dashed-double-dotted (orange), Nijm II + TM99 - double-dashed-dotted (maroon). All partial waves with 2N total angular momenta up to $j_{\text{max}} = 5$ have been included.

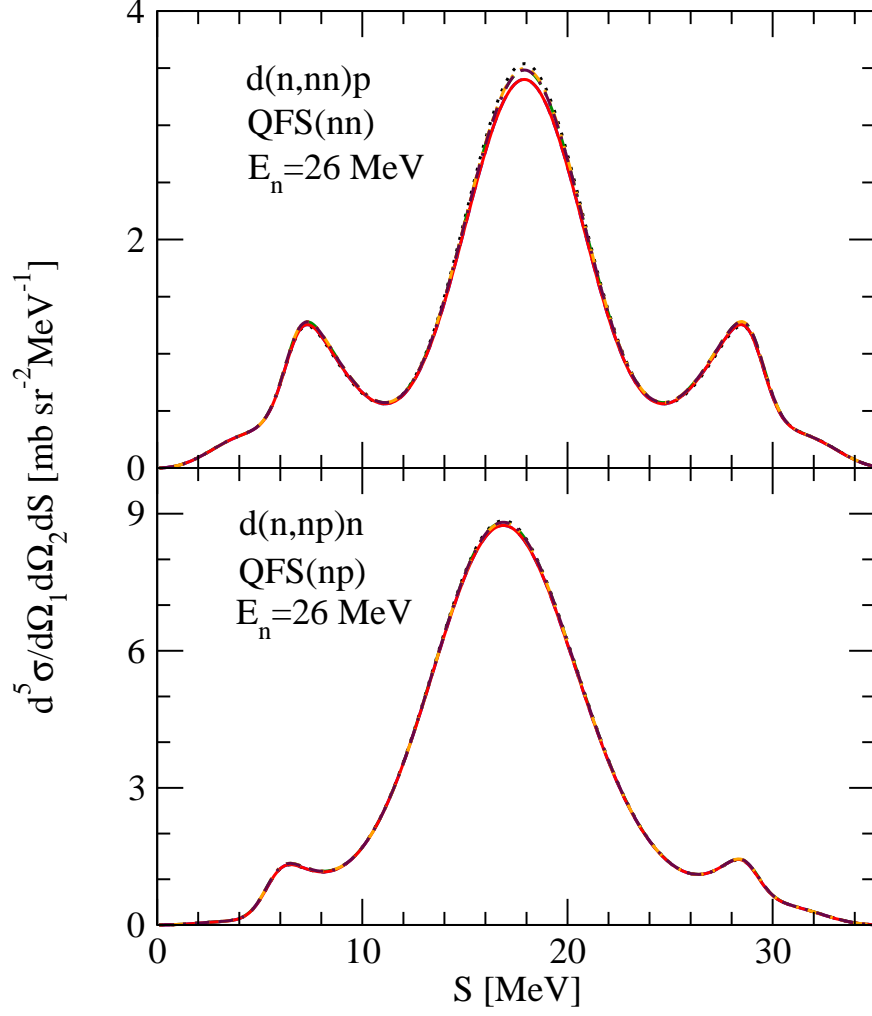


FIG. 2: (color online) The cross section $d^5\sigma/d\Omega_1 d\Omega_2 dS$ for the $E_n^{lab} = 26$ MeV nd breakup reaction $d(n, nn)p$ (upper panel) and $d(n, np)n$ (lower panel) as a function of the S-curve length for two complete configurations of Ref. [10]. QFS nn refers to the angles of two neutrons: $\theta_1 = \theta_2 = 42^\circ$ and QFS np refers to the angle $\theta_1 = 39^\circ$ of the detected neutron and $\theta_2 = 42^\circ$ for the proton. In both cases $\phi_{12} = 180^\circ$. For the description of lines see Fig. 1.

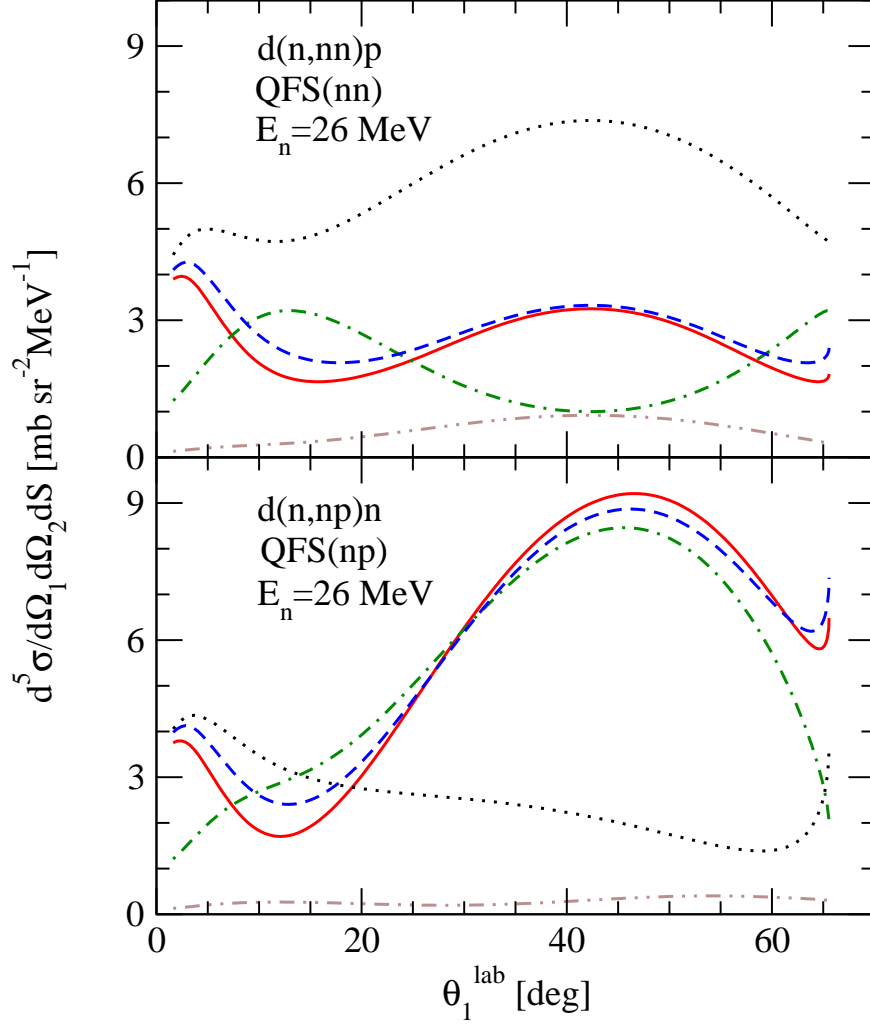


FIG. 3: (color online) The cross section $d^5\sigma/d\Omega_1 d\Omega_2 dS$ for the $E_n^{lab} = 26$ MeV nd breakup reaction $d(n, nn)p$ (upper panel) and $d(n, np)n$ (lower panel) under exact QFS condition (the momentum of the undetected third nucleon $\vec{p}_3^{lab} = 0$: nn QFS for the upper and np QFS for the lower panel) as a function of the laboratory angle of the detected neutron. The different lines show contributions from different NN force components. The solid (red) line is the full result based on the CD Bonn potential [24] and all partial waves with 2N total angular momenta up to $j_{max} = 5$ included. The dotted (black), dashed-dotted (green), and dashed (blue) lines result when only contributions from 1S_0 , $^3S_1 - ^3D_1$, and $^1S_0 + ^3S_1 - ^3D_1$ are kept when calculating the cross sections. The dashed-double-dotted (brown) line presents the contribution of all partial waves with the exception of 1S_0 and $^3S_1 - ^3D_1$.

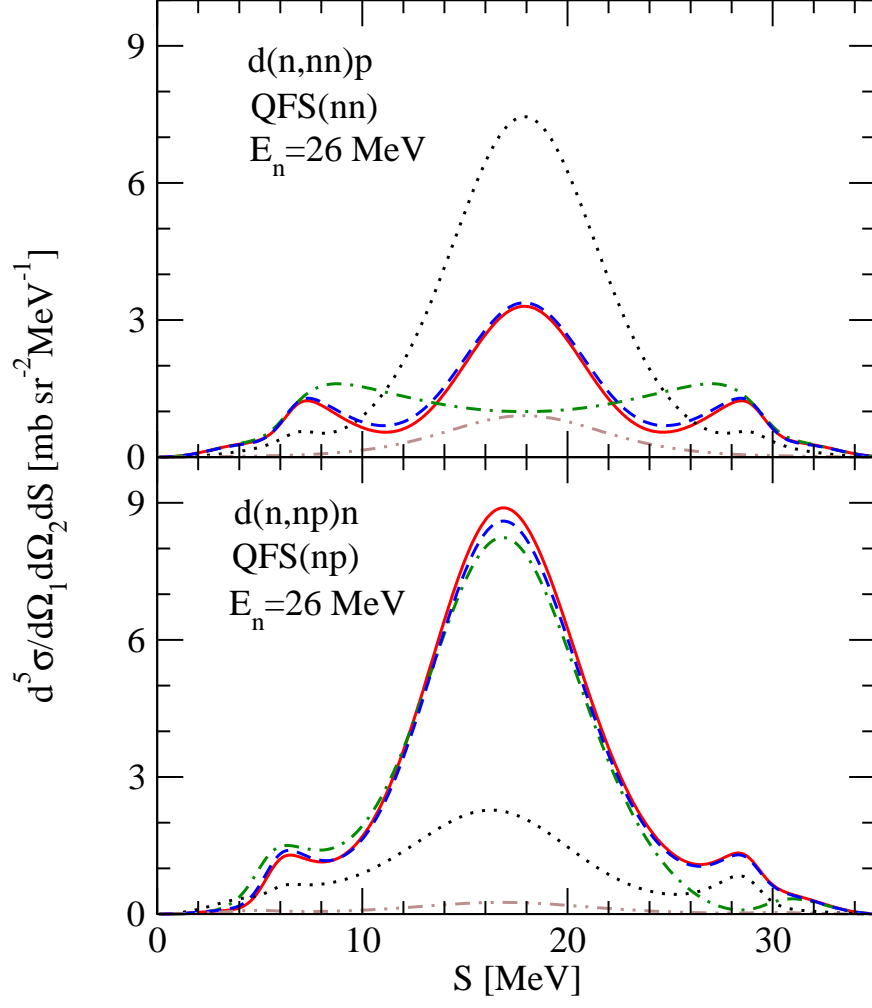


FIG. 4: (color online) The cross section $d^5\sigma/d\Omega_1 d\Omega_2 dS$ for the $E_n^{lab} = 26$ MeV nd breakup reaction $d(n,nn)p$ (upper panel) and $d(n,np)n$ (lower panel) as a function of the S-curve length for two complete configurations of Ref. [10]. QFS nn refers to the angles of two neutrons: $\theta_1 = \theta_2 = 42^\circ$ and QFS np refers to the angle $\theta_1 = 39^\circ$ of the detected neutron and $\theta_2 = 42^\circ$ for the proton. In both cases $\phi_{12} = 180^\circ$. For description of lines see Fig. 3.

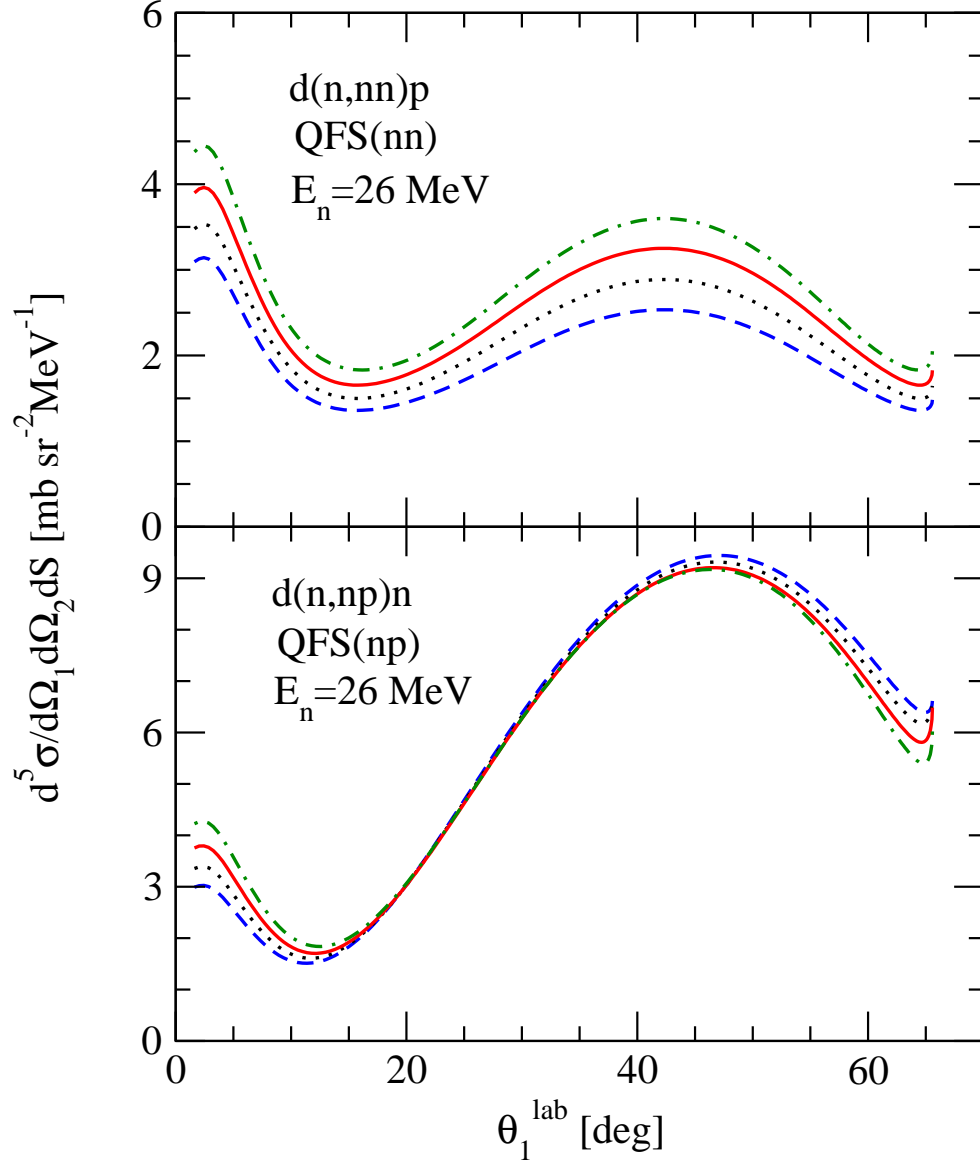


FIG. 5: (color online) The cross section $d^5\sigma/d\Omega_1 d\Omega_2 dS$ for the $E_n^{lab} = 26$ MeV nd breakup reaction $d(n, nn)p$ (upper panel) and $d(n, np)n$ (lower panel) under exact QFS condition (the momentum of the undetected third nucleon $\vec{p}_3^{lab} = 0$: nn QFS for the upper and np QFS for the lower panel) as a function of the laboratory angle of the detected neutron. The lines show the sensitivity of the QFS cross section to changes of the nn 1S_0 force component. Those changes were induced by multiplying the 1S_0 nn matrix element of the CD Bonn potential by a factor λ . The solid (red) line is the full result based on the original CD Bonn potential [24] and all partial waves with 2N total angular momenta up to $j_{max} = 5$ included. The dashed (blue), dotted (black), and dashed-dotted (green) lines correspond to $\lambda = 0.9, 0.95$, and 1.05 , respectively.

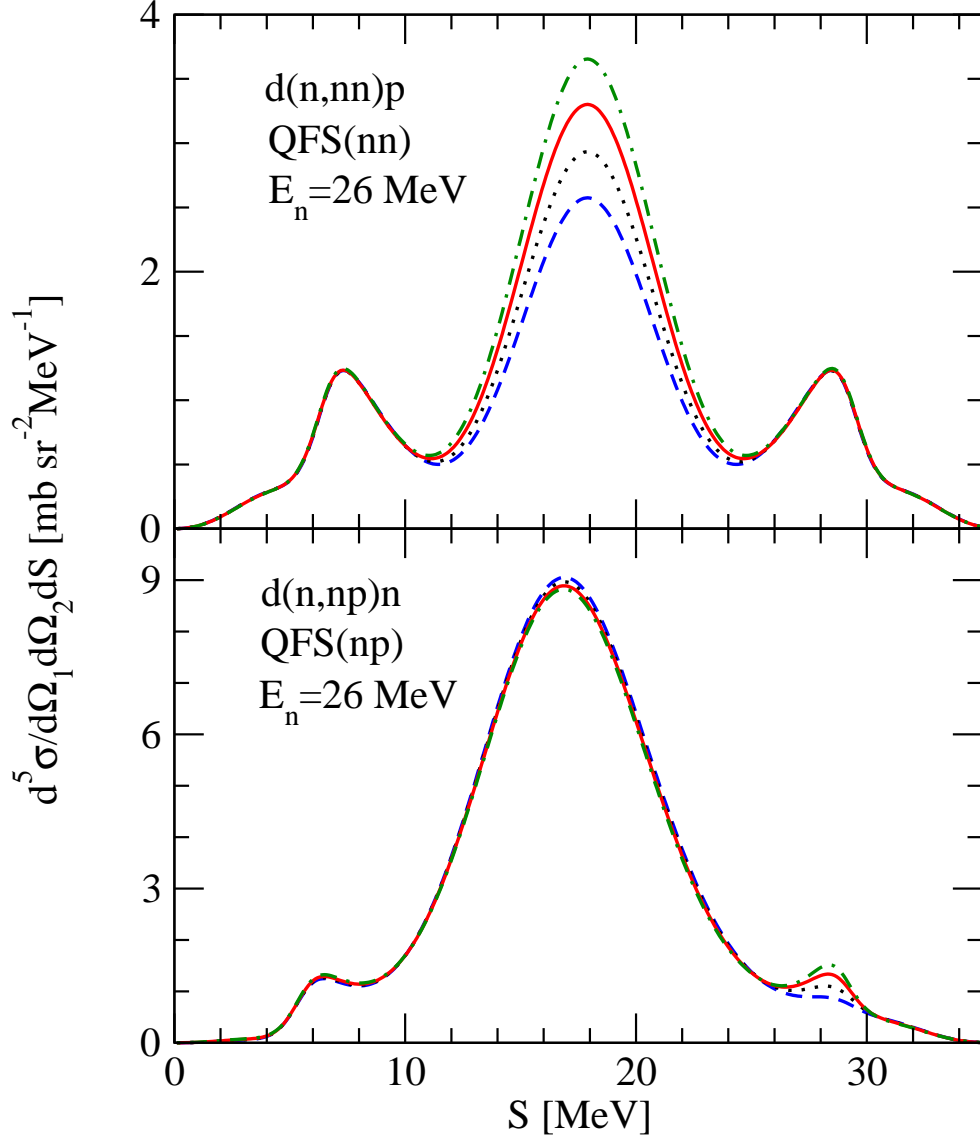


FIG. 6: (color online) The cross section $d^5\sigma/d\Omega_1 d\Omega_2 dS$ for the $E_n^{lab} = 26$ MeV nd breakup reaction $d(n, nn)p$ (upper panel) and $d(n, np)n$ (lower panel) as a function of the S-curve length for two complete configurations of Ref. [10]. QFS nn refers to the angles of two neutrons: $\theta_1 = \theta_2 = 42^\circ$ and QFS np refers to the angle of detected neutron $\theta_1 = 39^\circ$ and proton $\theta_2 = 42^\circ$. In both cases $\phi_{12} = 180^\circ$. For description of lines see Fig. 5.

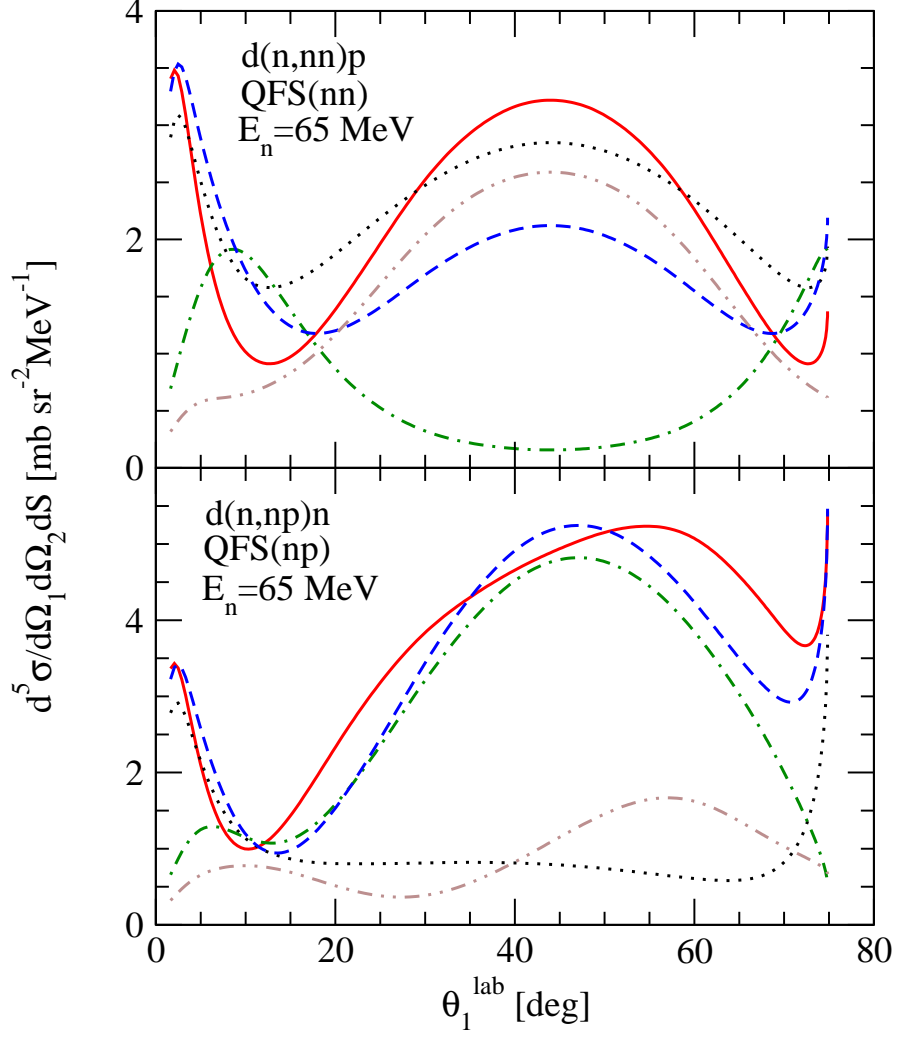


FIG. 7: (color online) The cross section $d^5\sigma/d\Omega_1 d\Omega_2 dS$ for the $E_n^{\text{lab}} = 65$ MeV nd breakup reaction $d(n,nn)p$ (upper panel) and $d(n,np)n$ (lower panel) under exact QFS condition (the momentum of the undetected third nucleon $\vec{p}_3^{\text{lab}} = 0$: nn QFS for the upper and np QFS for the lower panel) as a function of the laboratory angle of the detected neutron. The lines show contributions from different NN force components like in Fig.3.

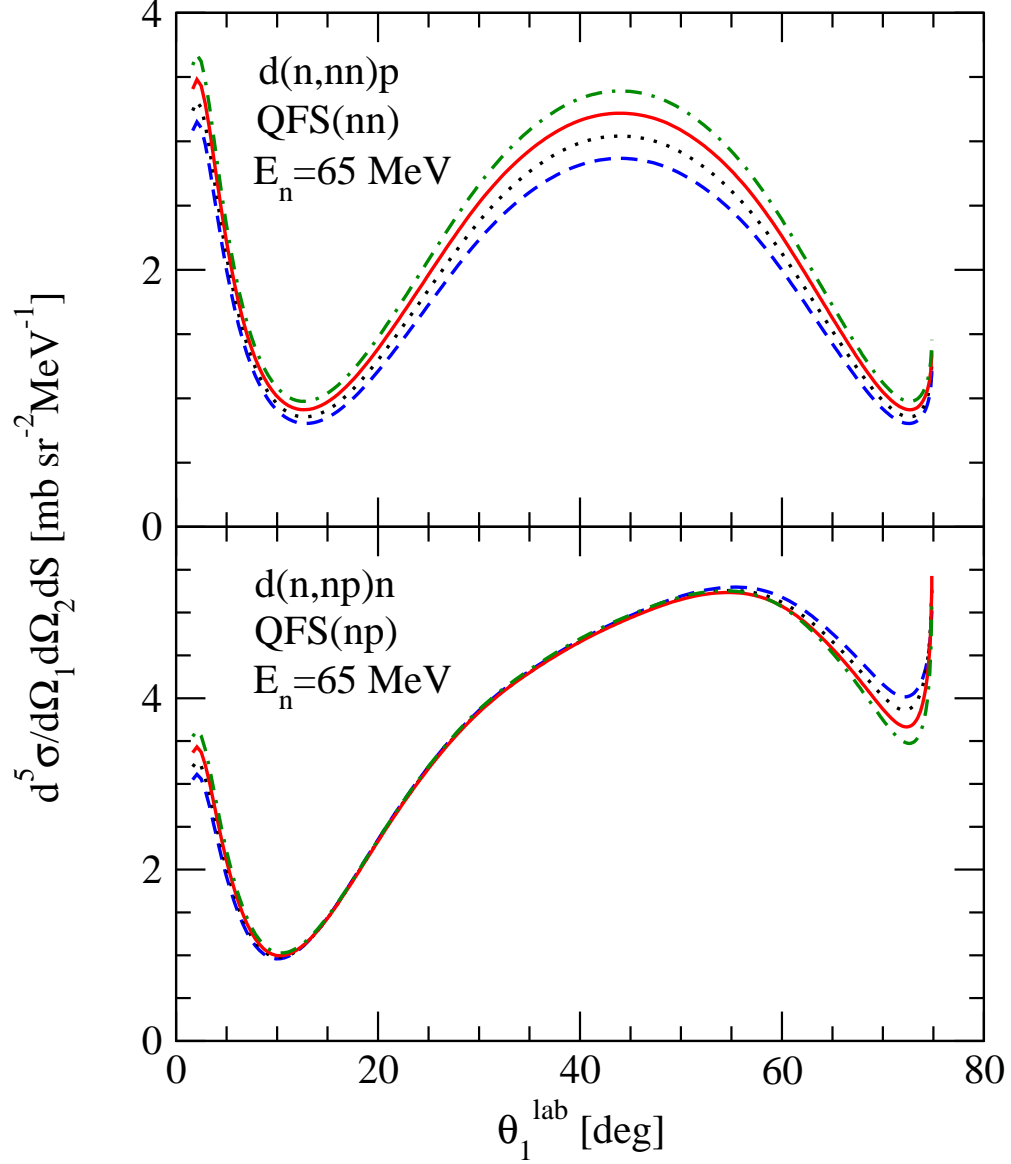


FIG. 8: (color online) The cross section $d^5\sigma/d\Omega_1 d\Omega_2 dS$ for the $E_n^{lab} = 65$ MeV nd breakup reaction $d(n, nn)p$ (upper panel) and $d(n, np)n$ (lower panel) under exact QFS condition (the momentum of the undetected third nucleon $\vec{p}_3^{lab} = 0$: nn QFS for the upper and np QFS for the lower panel) as a function of the laboratory angle of the detected neutron. The lines show sensitivity of the QFS cross section to the changes of the nn 1S_0 force component. Those changes were induced by multiplying the 1S_0 nn matrix element of the CD Bonn potential by a factor λ like in Fig.5.

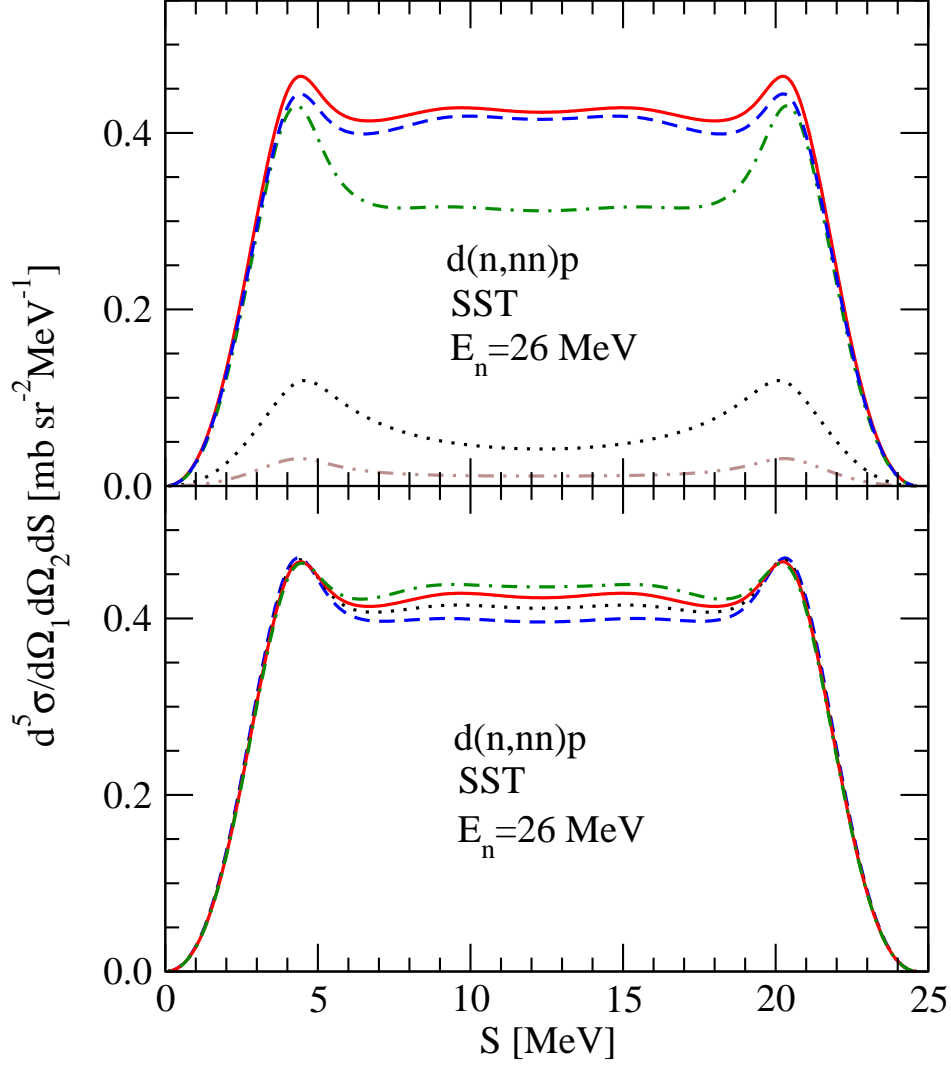


FIG. 9: (color online) The cross section $d^5\sigma/d\Omega_1 d\Omega_2 dS$ for the $E_n^{lab} = 26$ MeV nd breakup reaction $d(n,nn)p$ as a function of the S-curve length for SST configuration with the lab. angles of two detected neutrons $\theta_1 = \theta_2 = 52.8^\circ$ and $\phi_{12} = 180^\circ$. In the upper panel the lines show contributions from different NN force components. The solid (red) line is the full result based on the CD Bonn potential [24] and all partial waves with 2N total angular momenta up to $j_{max} = 5$ included. The dotted (black), dashed-dotted (green), and dashed (blue) lines result when only contributions from 1S_0 , $^3S_1 - ^3D_1$, and $^1S_0 + ^3S_1 - ^3D_1$ are kept when calculating the cross sections. The dashed-double-dotted (brown) line presents contribution of all partial waves with the exception of 1S_0 and $^3S_1 - ^3D_1$. In the lower panel the lines show sensitivity of the SST cross section to the changes of the nn 1S_0 force component. Those changes were induced by multiplying the 1S_0 nn matrix element of the CD Bonn potential by a factor λ . The solid (red) line is the full result based on the original CD Bonn potential [24] and all partial waves with 2N total angular momenta up to $j_{max} = 5$ included. The dashed (blue), dotted (black), and dashed-dotted (green) lines correspond to $\lambda = 0.9, 0.95$, and 1.05 , respectively.

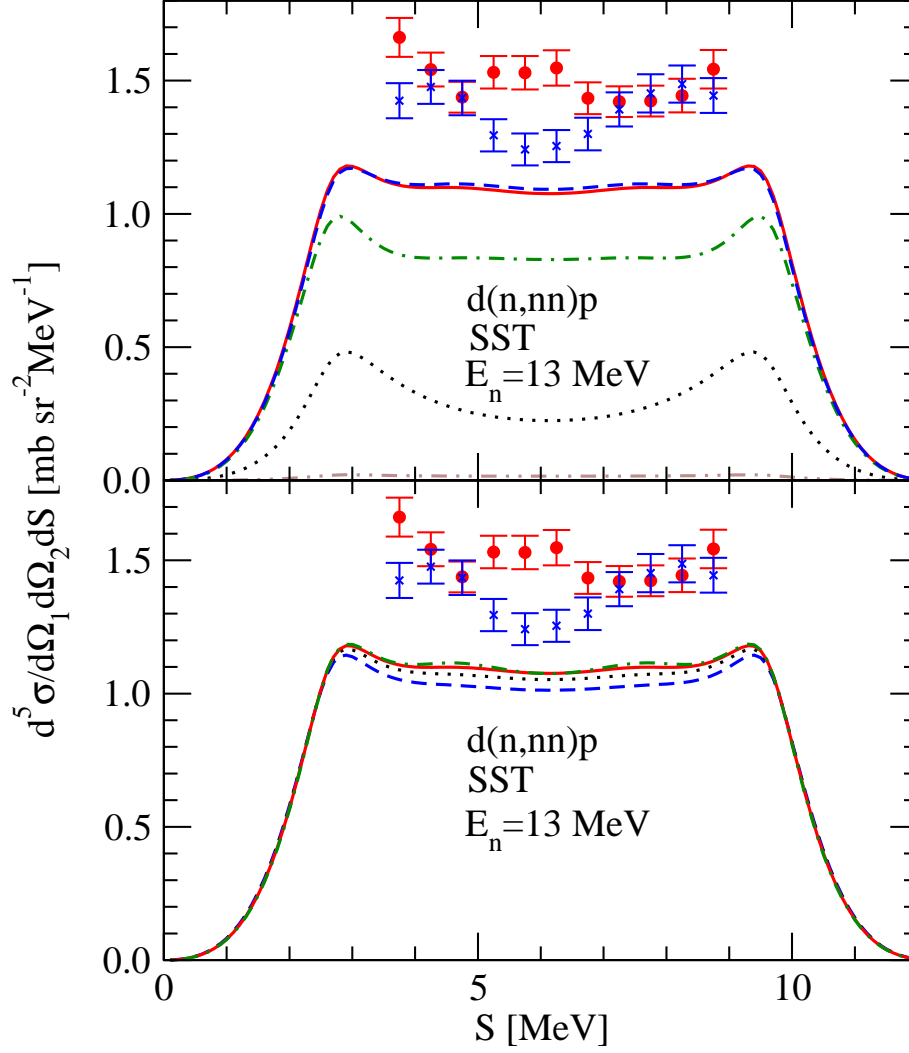


FIG. 10: (color online) The cross section $d^5\sigma/d\Omega_1 d\Omega_2 dS$ for the $E_n^{lab} = 13$ MeV nd breakup reaction $d(n,nn)p$ as a function of the S-curve length for SST configuration with the lab. angles of two detected neutrons $\theta_1 = \theta_2 = 50.5^\circ$ and $\phi_{12} = 180^\circ$. In the upper panel the lines show contributions from different NN force components. The solid (red) line is the full result based on the CD Bonn potential [24] and all partial waves with 2N total angular momenta up to $j_{max} = 5$ included. The dotted (black), dashed-dotted (green), and dashed (blue) lines result when only contributions from 1S_0 , $^3S_1 - ^3D_1$, and $^1S_0 + ^3S_1 - ^3D_1$ are kept when calculating the cross sections. The dashed-double-dotted (brown) line presents contribution of all partial waves with exception of 1S_0 and $^3S_1 - ^3D_1$. In the lower panel the lines show sensitivity of the SST cross section to the changes of the nn 1S_0 force component. Those changes were induced by multiplying the 1S_0 nn matrix element of the CD Bonn potential by a factor λ . The solid (red) line is the full result based on the original CD Bonn potential [24] and all partial waves with 2N total angular momenta up to $j_{max} = 5$ included. The dashed (blue), dotted (black), and dashed-dotted (green) lines correspond to $\lambda = 0.9, 0.95$, and 1.05 , respectively. The solid dots and x-ses are nd data of Ref. [7, 8] and [9], respectively.